

Merging Level 1 Ocean-Color Imagery from Multiple Sensors

Robert Frouin
*Scripps Institution of Oceanography
La Jolla, California*

MODIS/VIIRS Meeting, 26-28 January 2010, Washington, DC

References

Gross-Colzy, L., S. Colzy, R. Frouin, and P. Henry, 2007: A general ocean color atmospheric correction scheme based on principal component analysis - Part I: Performance on Case 1 and Case 2 waters. In *Coastal Ocean Remote Sensing*. Proceedings of SPIE, **6680**, doi: 10.1117/12.738508, 12 pp.

Gross-Colzy, L., S. Colzy, R. Frouin, and P. Henry, 2007: A general ocean color atmospheric correction scheme based on principal component analysis - Part II: Level 4 merging capabilities. In *Coastal Ocean Remote Sensing*. Proceedings of SPIE, **6680**, doi: 10.1117/12.738514, 12 pp.

Introduction

- Individual satellite ocean-color missions are limited in coverage by swath width and gaps caused by glint and clouds.
- Merging data from multiple sensors increases coverage of the products and improves statistical confidence in the data, facilitating the study of biological and physical phenomena.
- Current data-merging techniques start at the level of the water-leaving radiance or at the level of the derived products such as chlorophyll-a concentration.
- Difficult to deal properly with differences in radiometric calibration, atmospheric correction algorithm, solar and viewing angles, and individual product accuracies.

Approach

- To perform merging at the Level 1, using a scheme that accounts for differences in solar and viewing geometries and that is insensitive to radiometric calibration biases. Atmospheric correction is applied to the merged data.
- The scheme is based on principal component analysis of the TOA reflectance.
 - (1) For a common set of spectral bands, the principal components of the TOA reflectance vector are determined for each individual sensor.
 - (2) The components insensitive to angular geometry are selected, and respectively averaged over the various sensors.
 - (3) The averaged components are then mapped to the principal components of the marine reflectance, allowing a reconstruction of the marine reflectance.

Inversion scheme

$$\rho_p = \rho_{TOA} - \rho_m = f(\rho_w)$$

$$\rho_p = \sum_i c_{pi} e_{pi}$$

$$\rho_w = \sum_j c_{wj} e_{wj}$$

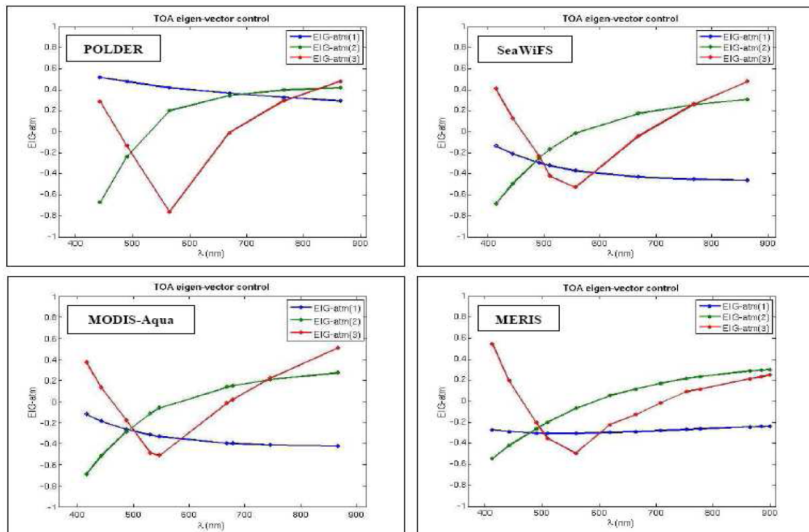
$$c_{wj} = g(c_{pi}'s) ?$$

-Whatever the atmospheric and surface conditions, the spectral shape of ρ_w imprints uniquely the spectral shape of ρ_p . The PCA algorithm extracts this imprint to retrieve ρ_w .

-The algorithm, therefore, is not sensitive to the absolute TOA reflectance level. The required information to retrieve ρ_w is not in the amplitude of ρ_p , but in its spectral shape.

-This makes the PCA algorithm robust to absolute calibration errors, a definite advantage compared with other techniques.

Eigenvectors of ρ_p



Eigenvectors of ρ_w

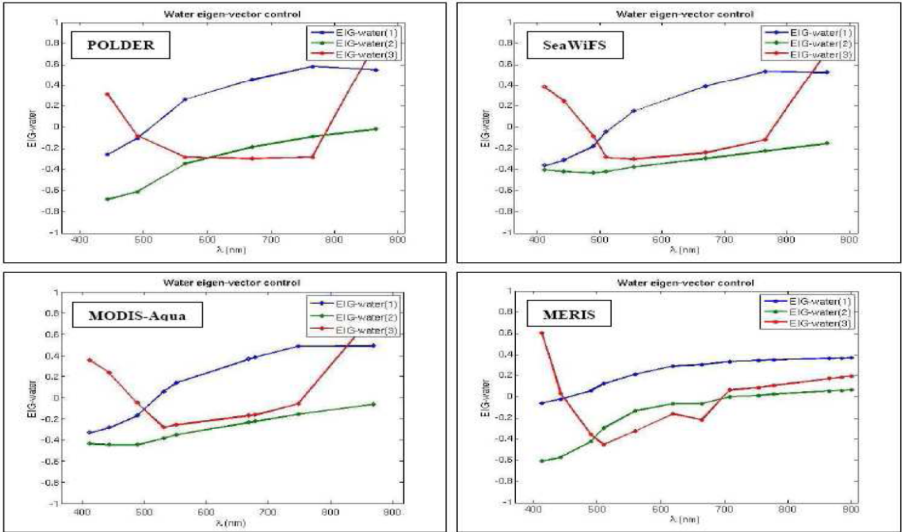


Figure 1: The first 3 eigenvectors of ρ_p (left) and ρ_w (right) for POLDER, SeaWiFS, MODIS-Aqua, and MERIS data ensembles. Spectral shapes are similar from one sensor to another, except for MERIS ρ_w because the data ensemble corresponds to a 3-component ocean model (chlorophyll, sediments, yellow substances) instead of a 1-component ocean model (chlorophyll).

- e_{p1} has smooth spectral shape (signal magnitude, ρ_a); e_{p1} has blue signature (multiple scattering, ρ_{ma}); strongly related to atmosphere and influenced by directionality, not used to retrieve ocean signal.

-Strong spectral shapes of e_{pi} , $i > 2$ are related to ocean color.

Table 1: Correlation coefficients between the principal components of ρ_p , c_{pi} , and of ρ_w , c_{wj} : Empirical functions based on linear correlation matrix; Canonical correlation k between desired c_{wj} and the set of c_{pi} selected to calculate it.

Sensor	Linear correlation matrix	Empirical functions	k (%)
POLDER	cp1 cp2 cp3 cp4 cp5 cp6 cw1 5.8 -39.1 -77.6 -25.8 -10.6 0.6 cw2 8.1 -10.8 24.3 -24.2 29.7 4.4 cw3 0.6 6.1 10.2 -58.4 24.5 -2.1	$cw1 = f(cp3, cp4, cp5)$ $cw2 = g(cp3, cp4, cp5)$ $cw3 = h(cp3, cp4, cp5)$	90.2 65.4 42.1
SeaWiFS	cp1 cp2 cp3 cp4 cp5 cp6 cp7 cp8 cw1 2.1 23.6 -59.4 -64.4 14.6 -13.2 -15.5 -4.5 cw2 10.8 7.0 36.7 -8.2 -27.5 -53.9 -57.3 -2.3 cw3 5.9 -12.7 31.3 -48.0 -54.1 39.6 13.5 -6.3	$cw1 = f(cp3, cp4, cp5, cp6, cp7)$ $cw2 = g(cp3, cp4, cp5, cp6, cp7)$ $cw3 = h(cp3, cp4, cp5, cp6, cp7)$	91.1 91.4 89.2
MODIS	cp1 cp2 cp3 cp4 cp5 cp6 cp7 cp8 cp9 cw1 0.5 23.7 -63.0 -64.6 -3.3 -1.3 -6.6 -2.0 4.2 cw2 11.0 8.2 35.7 -17.3 33.9 31.2 -60.9 -11.3 12.3 cw3 5.9 -12.4 28.0 -30.5 57.5 -44.8 27.6 1.0 -14.3	$cw1 = f(cp3, cp4, cp7)$ $cw2 = g(cp3, cp4, cp5, cp6, cp7, cp8)$ $cw3 = h(cp3, cp4, cp5, cp6, cp7)$	90.5 86.8 88.3
MERIS	cp1 cp2 cp3 cp4 cp5 cp6 cp7 cp8 cp9 cp10 cp11 cp12 cp13 cw1 -7.4 2.2 -72.6 -41.6 -23.4 -1.4 -3.2 -2.9 -1.2 -0.8 0.8 -0.4 -0.1 cw2 11.5 22.6 4.9 30.9 -9.0 -4.1 -18.9 0.0 -2.8 -3.0 -0.1 0.5 0.2 cw3 -0.4 1.1 18.1 27.8 -35.6 -5.7 6.5 0.6 -1.3 0.3 0.8 -0.4 0.1	$cw1 = f(cp3, cp4, cp5)$ $cw2 = g(cp3, cp4, cp5, cp6, cp7, cp9, cp10)$ $cw3 = h(cp3, cp4, cp5, cp6, cp7)$	86.6 38.0 49.1

-Functions f , g , and h approximated using multi-layered perceptrons.

Theoretical performance

Table 2: Mean theoretical performance for ρ_w estimated by the empirical functions f , g , and h (Table 1). Case of POLDER, SeaWiFS, and MODIS. Best results are obtained for SeaWiFS, which can be explained by the good spectral distribution of the 8 spectral bands.

Sensor name	Bands	RMS error	Relative error (%)	Linear Correlation (%)	Bias
Type of water					
POLDER	ρ_w (443)	0.0051	20	87	0.0011
extended Case 1 waters	ρ_w (490)	0.0026	15	85	0.0005
	ρ_w (565)	0.0022	15	93	0.0004
	ρ_w (670)	0.0007	23	93	0.0001
	ρ_w (765)	0.0004	29	92	0.0001
	ρ_w (865)	0.0002	26	92	0.0000
SeaWiFS	ρ_w (412)	0.0042	13	96	0.0009
extended Case 1 waters	ρ_w (443)	0.0030	12	96	0.0007
	ρ_w (490)	0.0021	11	93	0.0006
	ρ_w (510)	0.0014	9	92	0.0005
	ρ_w (555)	0.0014	9	96	0.0004
	ρ_w (670)	0.0003	12	98	0.0000
	ρ_w (765)	0.0001	17	97	0.0000
	ρ_w (865)	0.0001	17	97	0.0000
MODIS	ρ_w (412)	0.0049	17	95	0.0009
extended Case 1 waters	ρ_w (443)	0.0034	15	94	0.0006
	ρ_w (488)	0.0020	11	93	0.0005
	ρ_w (531)	0.0012	8	95	0.0002
	ρ_w (551)	0.0013	10	96	0.0000
	ρ_w (667)	0.0006	20	93	-0.0001
	ρ_w (678)	0.0005	21	93	-0.0001
	ρ_w (748)	0.0003	29	91	-0.0001
	ρ_w (869)	0.0001	27	92	0.0000

Table 2b: Mean theoretical performance for ρ_w estimated by the empirical functions f , g , and h (Table 1). Case of MERIS.

Sensor name		Bands	RMS error		Relative error (%)		Linear Correlation (%)		Bias	
Type of water										
Case 1 & Case 2 waters	MERIS	ρ_w (413)	0.0050	0.0053	26	17	95	96	0.0011	0.0023
		ρ_w (442)	0.0039	0.0035	21	17	95	94	0.0009	0.0009
		ρ_w (490)	0.0031	0.0023	16	14	97	70	0.0006	0.0003
		ρ_w (510)	0.0024	0.0018	14	12	98	89	0.0004	0.0004
		ρ_w (560)	0.0023	0.0014	14	12	99	97	0.0003	0.0003
		ρ_w (620)	0.0017	0.0008	20	18	97	95	0.0003	0.0000
		ρ_w (665)	0.0012	0.0005	21	19	97	94	0.0002	0.0000
		ρ_w (708)	0.0008	0.0004	24	21	96	93	0.0001	0.0000
		ρ_w (753)	0.0002	0.0001	25	23	96	93	0.0000	0.0000
		ρ_w (778)	0.0002	0.0001	26	23	96	93	0.0000	0.0000
		ρ_w (865)	0.0001	0.0001	28	25	96	93	0.0000	0.0000
		ρ_w (885)	0.0001	0.0001	29	26	96	93	0.0000	0.0000
		ρ_w (900)	0.0001	0.0000	29	26	96	93	0.0000	0.0000

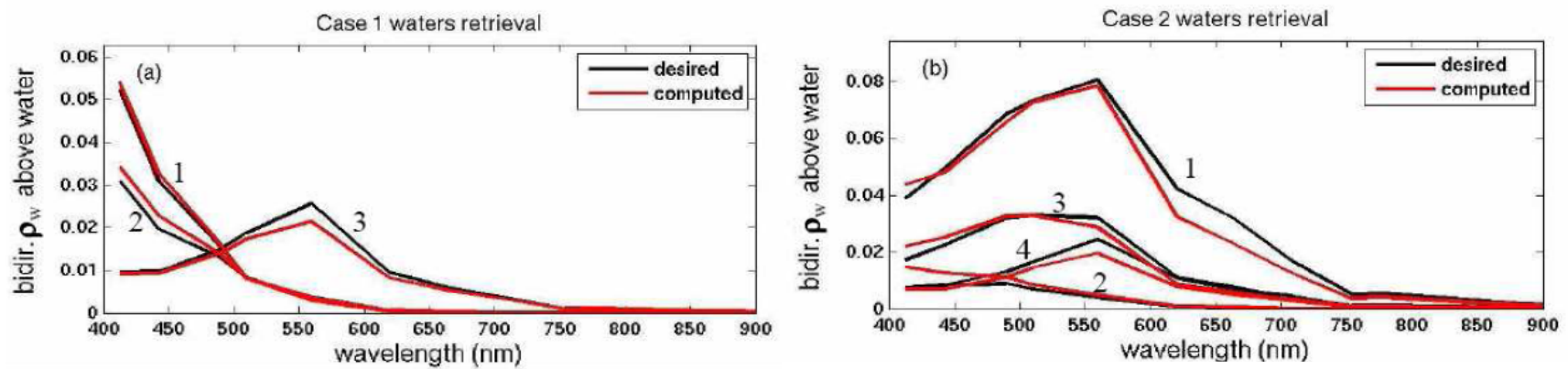


Figure 3: Examples of retrieved and desired ρ_w in case 1 and Case 2 waters.

Application to SeaWiFS imagery

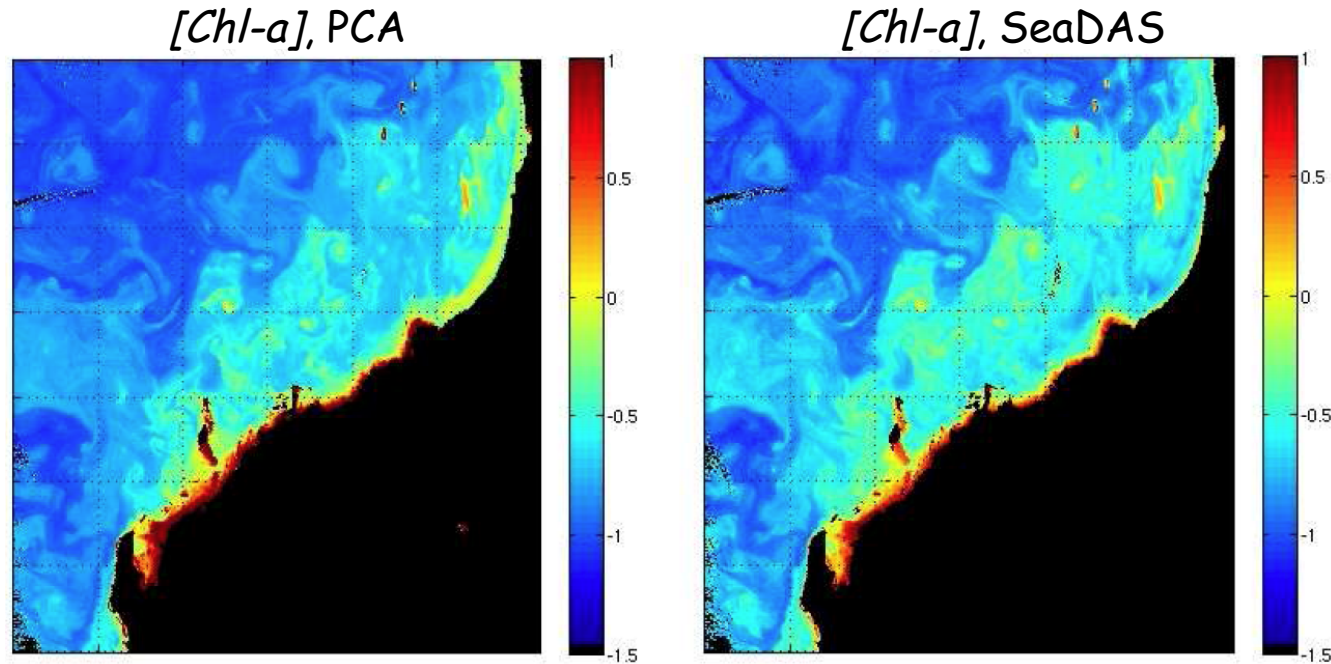


Figure 4: Chlorophyll-a concentration (log10 scale) off the Northwest coast of Australia, 21 August 2002, retrieved using the PCA method (left) and SeaDAS (right). Differences appear for small and large concentration values (higher dynamic range for PCA concentration).

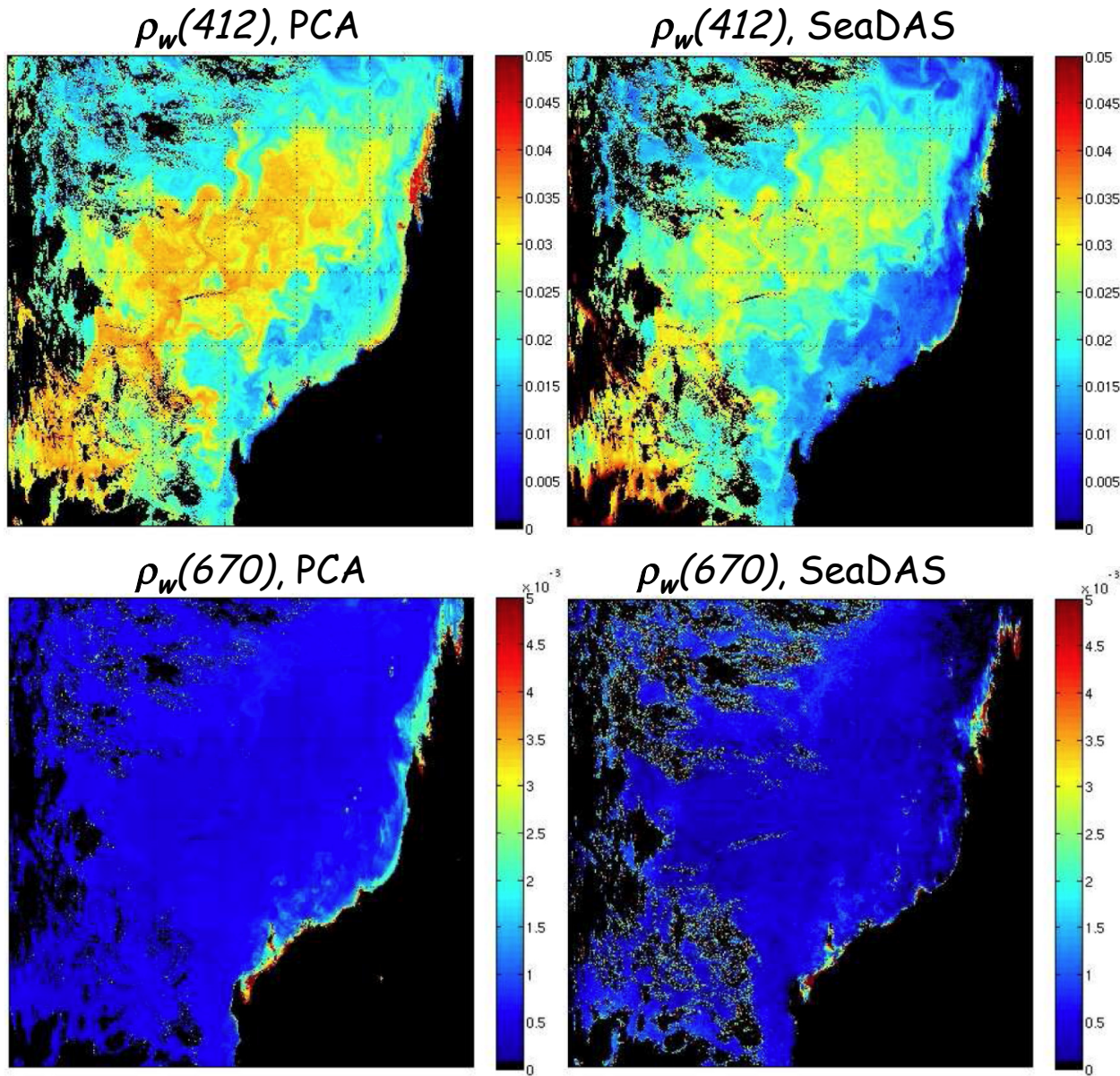


Figure 5: Marine reflectance retrieved using the PCA method (left) and SeaDAS (right). PCA reflectance is slightly higher in the blue. PCA imagery is less noisy.

Merging of POLDER imagery at multiple viewing angles

-The individual principal components c_{pki} of the n directional observations are weight-averaged:

$$c_{pi}(\text{merged}) = (1/\sum_k w_k) \sum_k w_k c_{pki}, \text{ with } k = 1, 2, \dots, n$$

where the weight w_k depends on the scattering angle.

-The quality of the merged product is quantified using a quality index QI :

$$QI = (1/n) \sum_k w_k, \text{ with } k = 1, 2, \dots, n$$

-Instead of using radiance reflectance, ρ_w , irradiance reflectance, R_w , is used.

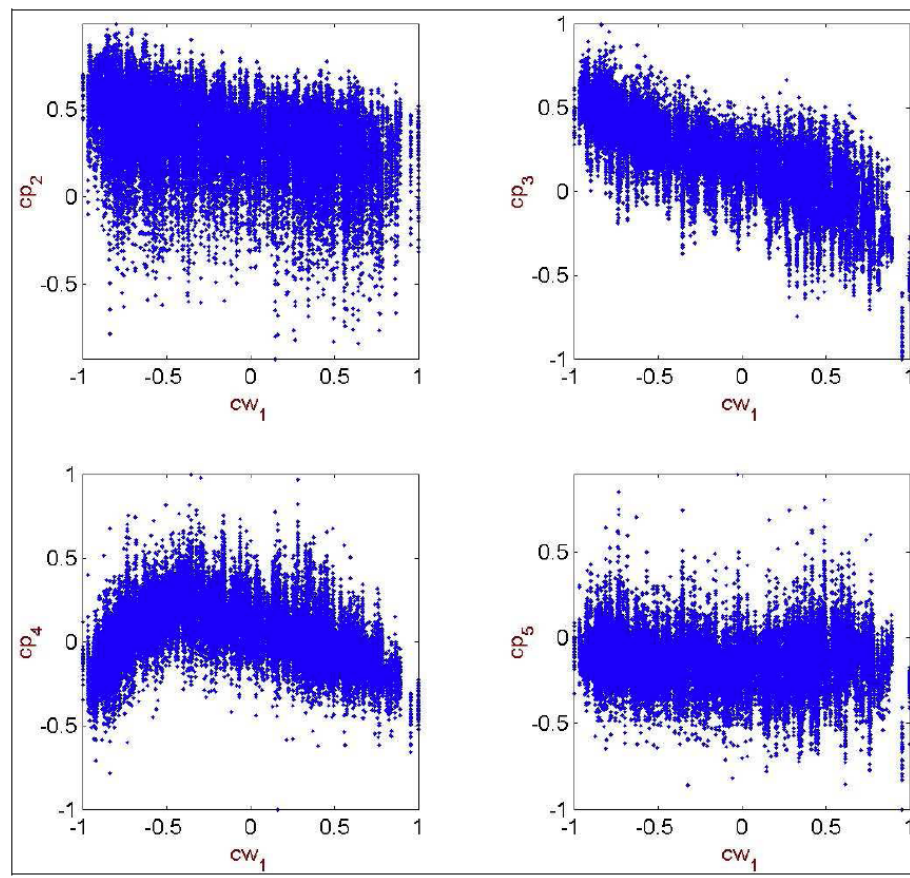


Figure 6: Relation between POLDER c_{w1} and c_{p2} , c_{p3} , c_{p4} , and c_{p5} (simulated data). The scatter of the data is partly due to directionality and c_{p2} is more subject to directionality than the other components.

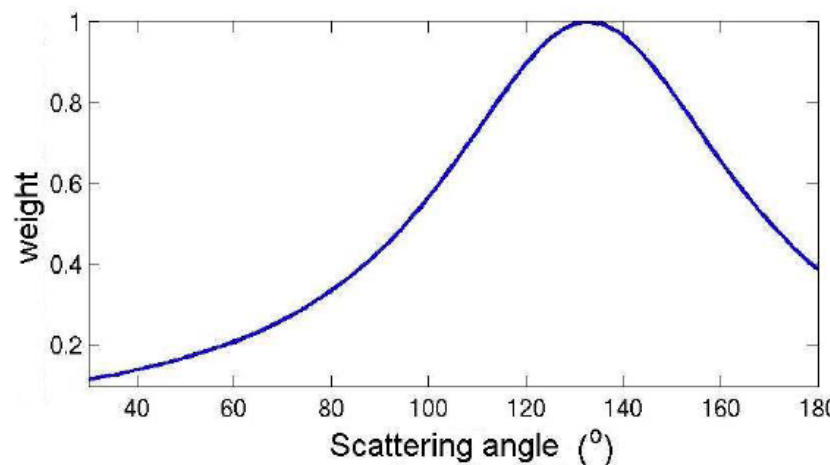


Figure 7: Weighting function for multi-directional merging of ρ_p principal components.

Table 3: Performance of the PCA method applied to POLDER simulated data (extended Case 1 waters). Marine reflectance R_w is computed from merged principal components.

Diffuse reflectance	Global RMS error	Global relative error (%)	Linear correlation (%)	Bias
$R_w(443)$	0.0044	18	90.1	0.0007
$R_w(490)$	0.0024	14	87.4	0.0004
$R_w(565)$	0.0019	14	95.0	0.0005
$R_w(670)$	0.0006	18	95.7	0.0002
$R_w(765)$	0.0003	23	94.8	0.0001
$R_w(870)$	0.0001	21	94.8	0.0000

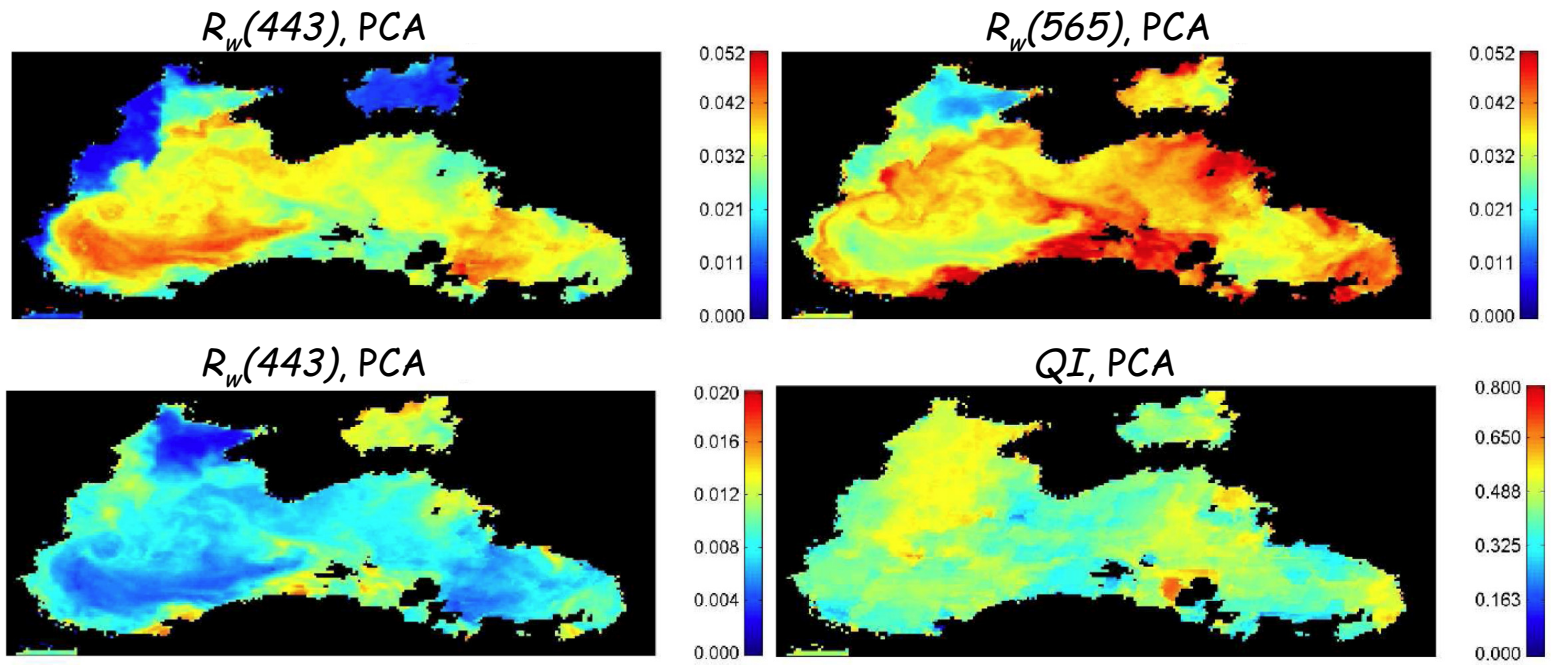


Figure 8: POLDER synthesis of marine reflectance for the first decade of June 2003, Black Sea, using the PCA method. (Upper left) $R_w(443)$. (Upper right) $R_w(565)$. (Lower left) $R_w(670)$, not retrieved by the standard POLDER algorithm. (Lower right) QI. Note that QI is not correlated to detected features.

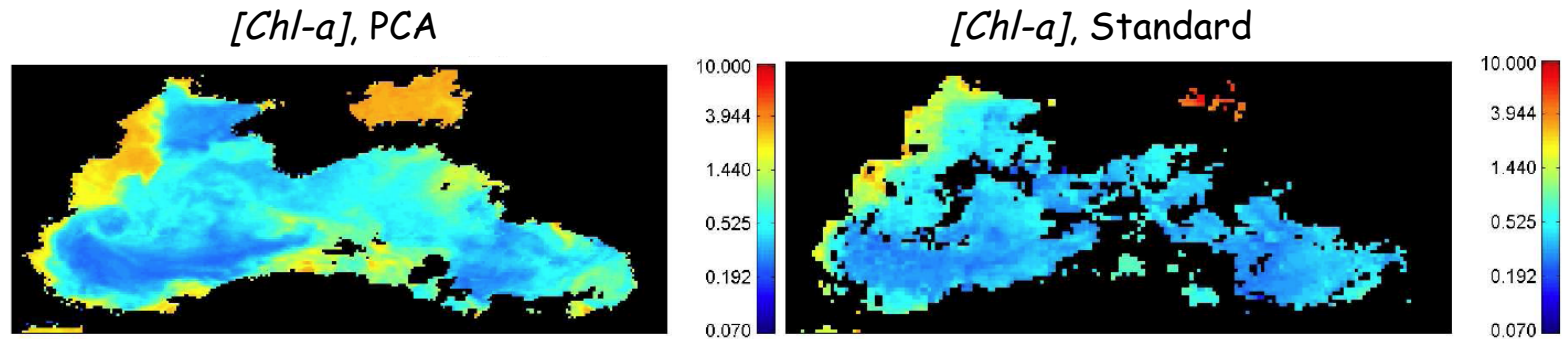


Figure 9: POLDER synthesis of of chlorophyll-a concentration for the first decade of June 2003, Black Sea. (Left) PCA method. (Right) Standard POLDER algorithm.

Merging of SeaWiFS and MODIS imagery

- Common set of spectral bands: SeaWiFS bands at 412, 443, 490, 555, 670, 765, and 865 nm; MODIS data at 488, 531, 551, 667, 678, 748, and 869 are interpolated to the SeaWiFS bands.
- Co-registered c_p s are merged and MLPs applied to the merged c_p s.

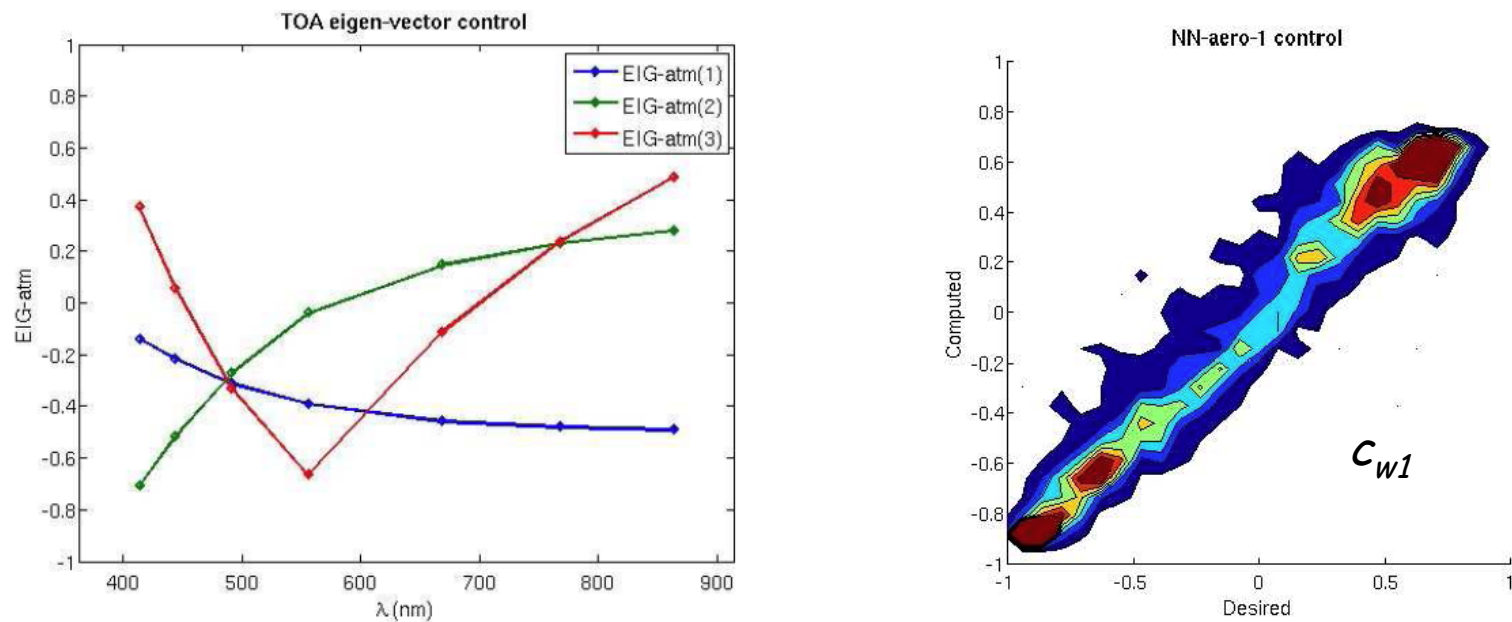


Figure 10: (Right) First 3 basis vectors of p_p . (Left) Estimated versus desired c_{w1} (first component of R_w). This component is estimated from c_{p3} , c_{p4} , and c_{p5} with a mean accuracy of about 3% and a correlation coefficient of 90%.

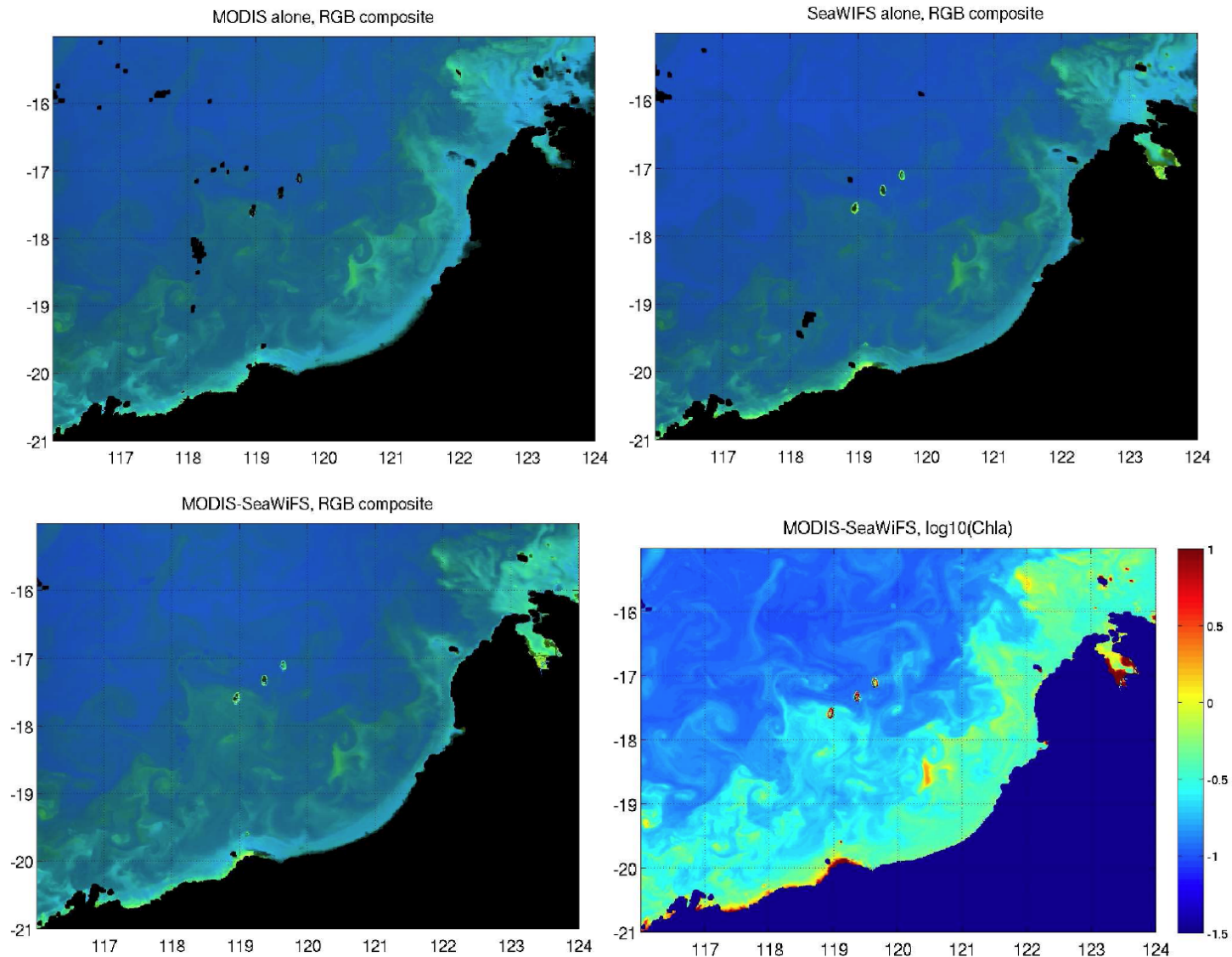


Figure 11: RGB composites (443, 555, and 670 bands) of R_w and $[CHL-a]$ (\log_{10} scale) obtained with the PCA algorithm. Imagery was acquired off Northwest Australia, 21 August 2002.

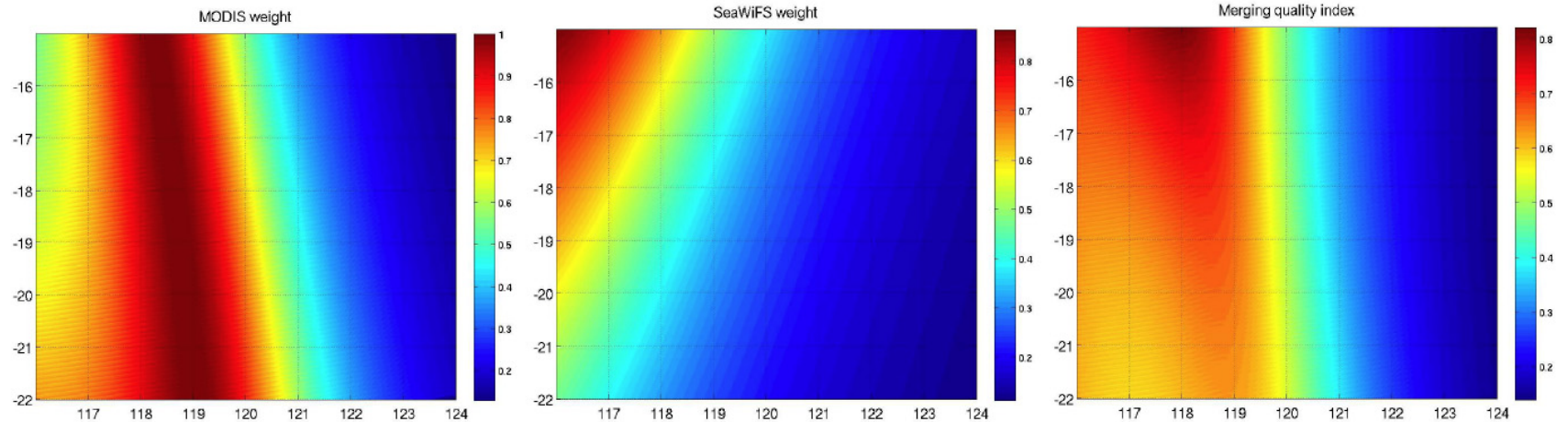


Figure 12: (Left) and (Middle) MODIS and SeaWiFS weights w_k . (Right) Merging quality index, QI. The merging process makes more pixels close to the MLP regression centers (the closer to 1, the better), which improves the accuracy of the retrieved geophysical parameters.

Summary

- Atmospheric correction of satellite ocean color imagery can be achieved effectively by decomposing the TOA signal into principal components and selecting the components sensitive to the ocean signal.
- By operating with principal components the PCA algorithm is minimally affected by biases in radiometric calibration (only inter-band calibration needs to be accurate), making it well adapted to provide consistency across sensors and continuity in the quality of the marine reflectance.

Summary (cont.)

- The PCA algorithm was tested theoretically on 4 ocean color sensors with increasing spectral accuracy. The more spectral bands, the more variability in the ocean signal can be retrieved.
- The PCA algorithm is able to perform atmospheric correction for varied water types, because the black-pixel assumption is not necessary.
- Level 1 merging ability of the PCA algorithm was demonstrated on POLDER multi-directional imagery and with MODIS and SeaWiFS imagery.